AMERICAN SOCIETY FOR MICROBIOLOGY | Infection and Immunity®

CELLULAR MICROBIOLOGY:
PATHOGEN-HOST CELL MOLECULAR INTERACTIONS

Control of Mucosal Candidiasis in the Zebrafish Swim Bladder Depends on Neutrophils That Block Filament Invasion and Drive Extracellular-Trap Production

Remi L. Gratacap,[a] Allison K. Scherer,[a] Brittany G. Seman,[a] Robert T. Wheeler[a,b]

Department of Molecular & Biomedical Sciences, University of Maine, Orono, Maine, USA[a]; Graduate School of Biomedical Sciences and Engineering, University of Maine, Orono, Maine, USA[b]

ABSTRACT *Candida albicans* is a ubiquitous mucosal commensal that is normally prevented from causing acute or chronic invasive disease. Neutrophils contribute to protection in oral infection but exacerbate vulvovaginal candidiasis. To dissect the role of neutrophils during mucosal candidiasis, we took advantage of a new, transparent zebrafish swim bladder infection model. Intravital microscopic tracking of individual animals revealed that the blocking of neutrophil recruitment leads to rapid mortality in this model through faster disease progression. Conversely, artificial recruitment of neutrophils during early infection reduces disease pressure. Noninvasive longitudinal tracking showed that mortality is a consequence of *C. albicans* breaching the epithelial barrier and invading surrounding tissues. Accordingly, we found that a hyperfilamentous *C. albicans* strain breaches the epithelial barrier more frequently and causes mortality in immunocompetent zebrafish. A lack of neutrophils at the infection site is associated with less fungus-associated extracellular DNA and less damage to fungal filaments, suggesting that neutrophil extracellular traps help to protect the epithelial barrier from *C. albicans* breach. We propose a homeostatic model where *C. albicans* disease pressure is balanced by neutrophil-mediated damage of fungi, maintaining this organism as a commensal while minimizing the risk of damage to host tissue. The unequaled ability to dissect infection dynamics at a high spatiotemporal resolution makes this zebrafish model a unique tool for understanding mucosal host-pathogen interactions.

KEYWORDS *Candida albicans*, mucosal immunity, neutrophils, zebrafish

Candida albicans is the most successful commensal fungus at causing opportunistic mucosal and invasive infections (1, 2). The opportunistic nature of *C. albicans* mucosal infection suggests that there is a constantly challenged impasse between our immune defenses and *C. albicans* virulence factors (3, 4). Chronic mucocutaneous candidiasis (CMC) is associated with inborn errors of adaptive immune pathways, especially Th17 immunity (5). However, acute oropharyngeal candidiasis (OPC) is more common in neutropenic patients and can result from a multitude of immune-suppressive treatments that affect both innate and adaptive immunity, such as radiation/chemotherapy and corticosteroid or antibiotic use (6, 7).

Experimental work in murine models of OPC suggests that *C. albicans* is kept at bay in mucosal tissues through the action of epithelial cells, neutrophils, and macrophages (8). To protect from mucosal invasion in OPC, neutrophils must be present in the blood, be recruited to the site of infection, and possess a fully functional antimicrobial arsenal (9–12). Neutrophils attack both the yeast and filamentous forms of *C. albicans* and are associated with vulvovaginal candidiasis (13–15). Counterintuitively, because symptomatic infection is more closely associated with high neutrophil numbers than with the fungal burden, it is believed that neutrophils do more to cause infection symptoms

Received 21 April 2017 **Returned for modification** 10 May 2017 **Accepted** 5 June 2017

Accepted manuscript posted online 12 June 2017

Citation Gratacap RL, Scherer AK, Seman BG, Wheeler RT. 2017. Control of mucosal candidiasis in the zebrafish swim bladder depends on neutrophils that block filament invasion and drive extracellular-trap production. Infect Immun 85:e00276-17. https://doi.org/10.1128/IAI.00276-17.

Editor George S. Deepe, University of Cincinnati

Address correspondence to Robert T. Wheeler, robert.wheeler1@maine.edu.

This article is Maine Agricultural and Forest Experiment Station publication number 3481.

than prevent disease in the vaginal cavity (4, 15, 16). These contrasting activities in different tissues demonstrate that the actions of neutrophils at the site of infection can be vital for defense but must nevertheless be kept under tight control. Since immunosuppression and immunomodulation strategies are used for the treatment of many conditions, such as autoimmune diseases, cancers, or infections, determination of the protective elements of the immune response to mucosal infection is critical for improving care in many patient populations.

We do not yet understand the protective functions of neutrophils at the site of mucosal infection, such as how they control the infection or how reduced numbers or the limited activity of neutrophils induces susceptibility at the site of mucosal infection. One way in which neutrophils deal with organisms that are too large to be phagocytosed is through the production of neutrophil extracellular traps (NETs) (17). NETs have been shown to inhibit both yeast and hyphae (15) but are preferentially released against *C. albicans* hyphae (17). While it is not yet proven, a role for NETs in protection against mucosal candidiasis has been proposed because extracellular traps are present in mucosal murine infections and because phagocyte oxidase-deficient mice that do not produce NETs are more susceptible to OPC (12, 17, 18). Despite this circumstantial evidence, it has been difficult to determine the source of these extracellular traps, their effects on *C. albicans* cells during infection, and whether they play a definitive role in protection.

The mucosal infection strategy of *C. albicans* is believed to include induced endocytosis of filaments; production of lytic enzymes, such as secreted aspartyl proteases and candidalysin; invasion and tissue damage by hyphae; and spread within the blood by yeast (19–23). However, it is not clear which of these activities is crucial in directing invasive mucosal disease *in vivo* and how the innate immune system prevents colonization of sterile tissues under homeostatic conditions. Testing the *in vivo* relevance of mechanisms defined *in vitro* is technically challenging in the mouse, but this major knowledge gap has been successfully filled in a number of cases by modeling with the transparent zebrafish larva (24).

The zebrafish larva is a simplified model organism that combines the advantages of high-resolution imaging available *in vitro* with an examination of infection dynamics *in vivo* with a vertebrate immune system and has been useful in studying bacterial, viral, fungal, and parasitic infections (25, 26). We recently developed the first microinjection mucosal infection model in the zebrafish larva, and it has been used to study sterile inflammation and infection with both viral and fungal pathogens (27–29). In this study, we leveraged this infection model to achieve a high spatiotemporal resolution of neutrophil-*C. albicans* dynamics at the mucosal level. We show that, similarly to the murine model of OPC, neutrophils are important in protection against mucosal candidiasis. Our longitudinal dissection of infection dynamics in individual animals highlights a conserved role of neutrophil recruitment in protection, suggesting that neutrophils prevent epithelial tissue invasion by directly impacting the pathogen burden. We also found that *C. albicans* filamentation is an integral component of this pathogen's invasion strategy and show that neutrophils are important for damage of fungal filaments and extracellular-trap formation. These data show that the zebrafish swim bladder platform is a unique and powerful mucosal infection model for directly imaging the role of the *C. albicans* morphotype in breaching the host epithelial layer, the response of innate immune cells, and the consequences of a lack of specific immune cell types at the single-cell level.

RESULTS

Neutrophils and conserved chemotactic pathways are essential for mucosal immunity to candidiasis in the zebrafish swim bladder. Neutrophils and macrophages are the first professional immune cells to respond to infection and are associated with protection against oral *C. albicans* infections (30). In this study, we sought to determine the roles of these phagocytes in protection against mucosal candidiasis in the context of *C. albicans* infection in the juvenile zebrafish swim bladder. The swim

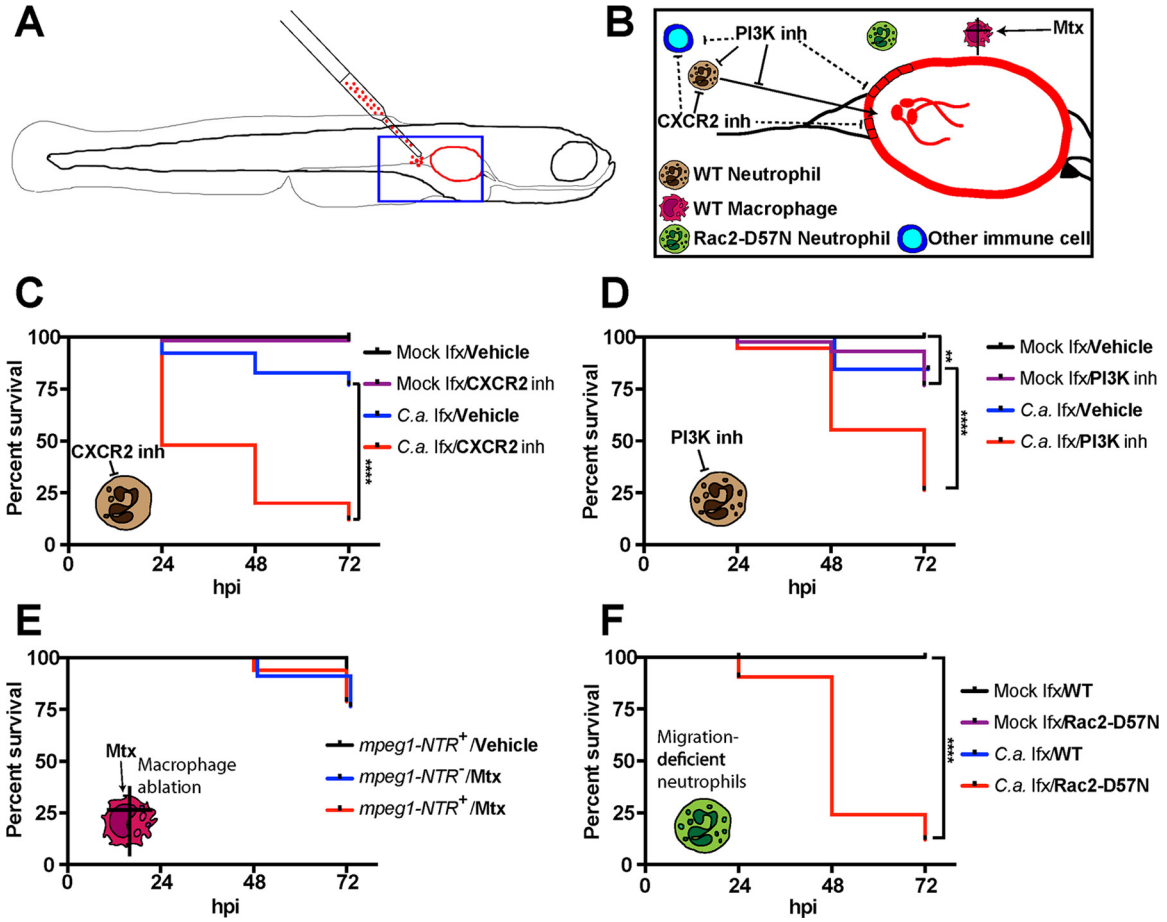

FIG 1 Neutrophils but not macrophages protect against death in the zebrafish mucosal candidiasis model. (A) Diagram of the swim bladder injection model used in this study. (B) Schematic of the strategy used to test the role of neutrophils and macrophages in protection against mucosal candidiasis. (C to F) At 4 days postfertilization (dpf), zebrafish of the wild-type (WT) (C and D), *mpeg1-NTR* (E), and *mpo*:*Rac2-D57N* (F) lines were infected with 4 nl of Caf2-dTomato (Caf2-dTom) yeast cells (3×10^7 CFU/ml in 5% polyvinylpyrrolidone [PVP]) or with PVP only. Fish were incubated in different chemical inhibitors (B) for an hour prior to injection: the CXCR2 inhibitor SB225002 at 2 μg/ml or 0.02% DMSO (C), the pan-PI3K inhibitor LY294002 at 5 μg/ml or 0.05% DMSO (D), or metronidazole (Mtx) at 20 mM (E). Fish were screened immediately after injection, and only fish with 50 to 100 yeast cells in the inoculum in the swim bladder were selected. Fish were returned to the chemical inhibitor or vehicle (C and D) at the same concentration or to Mtx (5 mM) (E), and survival was monitored daily for 3 days. Data pooled from three independent experiments are represented and were analyzed by the Kaplan-Meier test. Data are for 56, 57, 52, and 50 fish for the four groups indicated from top to bottom, respectively, in the key to panel C; 40, 43, 32, and 38 fish for the four groups indicated from top to bottom, respectively, in the key to panel D; 42, 34, and 33 fish for the three groups indicated from top to bottom, respectively, in the key to panel E; and 50, 53, 52, and 55 fish for the four groups indicated from top to bottom, respectively, in the key to panel F. Log-rank (Mantel-Cox) statistical tests showed that the results for fish infected with *C. albicans* and treated with an inhibitor (*C.a.* infection [Ifx]/inhibitor [inh]) and fish infected with *C. albicans* and treated with the vehicle (*C.a.* Ifx/Vehicle) or fish mock infected and treated with a CXCR2 inhibitor (Mock Ifx/CXCR2 inh) were significantly different ($P < 0.0001$) in panels C, D, and F but not in panel E. By the same test, in panel D, the results for fish mock infected and treated with the vehicle (Mock Ifx/Vehicle) were significantly different from those for fish mock infected and treated with the PI3K inhibitor (Mock Ifx/PI3K inh) ($P = 0.0013$). **, $P < 0.01$; ****, $P < 0.0001$.

bladder is an organ roughly homologous to the mammalian lung (31, 32). Composed as a single layer of epithelial cells covered by mucus that interacts with air and overlies a mesodermal layer, this organ is a suitable simplified model with which to study mucosal candidiasis (33). The infection is initiated by injecting *C. albicans* directly in the swim bladder lumen (Fig. 1A), and immunocompetent fish control a moderate infection inoculum (up to 50 organisms) so that mortality is rare over the first 3 days of infection (28).

We first tested the protective role of innate immune cells by either perturbing the signaling pathways that we predicted would be required for neutrophil recruitment or chemically ablating macrophages using the nitroreductase system (Fig. 1B). Chemical inhibition of the activity of CXCR2, a major CXC cytokine receptor highly expressed on

the surface of neutrophils, limits their recruitment to bacterial infection in zebrafish larvae and increases susceptibility to mucosal candidiasis in a murine model (11, 34). In *C. albicans* swim bladder infection, CXCR2 inhibition led to a dramatic increase in mortality from mucosal candidiasis compared to that in mock-infected fish as well as vehicle (dimethyl sulfoxide [DMSO])-treated infected animals (Fig. 1C). Over half of the fish in which CXCR2 was inhibited succumbed to the infection within the first 24 h postinfection (hpi), pointing to an evolutionarily conserved role of this chemokine receptor in protection against *C. albicans* mucosal infection in vertebrates. The pan-phosphatidylinositol 3-kinase (PI3K) inhibitor LY294002 also inhibits the recruitment of neutrophils to the site of bacterial infection in zebrafish larvae (34). Similarly, we found that inhibition of PI3K signaling led to a strong increase in susceptibility to *C. albicans* infection, with more than 70% of the animals succumbing to the infection by 72 hpi (Fig. 1D). It is important to note that this signaling pathway is involved in cellular homeostasis, which might explain why a small but statistically significant number of uninfected, inhibitor-treated animals also succumbed by 72 hpi. PI3K inhibition has also been shown to reduce cytokine production in epithelial cells after *C. albicans* infection (35). Thus, these inhibitors may be doing more than simply blocking neutrophil recruitment.

In fact, when neutrophil numbers were measured at 24 hpi, we found that PI3K inhibition caused lower levels of recruitment (see Fig. S1A in the supplemental material), but CXCR2 inhibition, surprisingly, did not decrease the level of recruitment (Fig. S1B). We repeated these experiments at earlier time points to check for subtle recruitment differences, but CXCR2 inhibition did not affect neutrophil recruitment at 4 or 8 hpi (Fig. S1C). Interestingly, while we confirmed that early neutrophil recruitment to the otic vesicle upon bacterial infection was CXCR2 dependent, there was no early neutrophil recruitment to the site of *C. albicans* infection in the otic vesicle (Fig. S2). We noted that, as previously published, a small amount of neutrophil recruitment could result from damage associated with the microinjection procedure itself (36). The results of these inhibitor experiments suggest that signaling proteins known to be important in neutrophil chemotaxis and function are crucial for resistance to mucosal candidiasis in the zebrafish swim bladder but act through different mechanisms. However, the use of chemical inhibitors suffers from the drawback that small-molecule inhibitors can have important off-target effects. Additionally, the pathways investigated exist in multiple cell types, so the possibility that other immune cell types, such as macrophages, play a role cannot be ruled out.

Testing the contribution of macrophages in immunity to mucosal disease has been particularly problematic in mammalian models, in part due to difficulties in eliminating tissue macrophages. Using a transgenic line of fish in which macrophages express a fusion of the bacterial nitroreductase (NTR) gene to the mCherry fluorescent protein and the addition of the protoxin metronidazole (Mtx), it is possible to efficiently ablate macrophages during fungal infection (24, 37). While metronidazole had some limited toxicity on its own in the absence of nitroreductase-expressing cells, no additional mortality was observed after ablation of nitroreductase-expressing macrophages (Fig. 1E). We also tested the possibility that the CXCR2 inhibitor might in part enhance the susceptibility to infection by limiting macrophage recruitment. On the contrary, the increased burden of infection upon CXCR2 inhibition apparently stimulated slightly increased levels of macrophage recruitment (Fig. S3). The results of these experiments suggest that macrophages play a largely redundant role in protection against invasive *C. albicans* mucosal infection in this model.

To complement these chemical inhibition experiments, we exploited a neutrophil-specific genetic tool to test the role of neutrophil recruitment in resistance to swim bladder infection. We used a fish line developed in the laboratory of Anna Huttenlocher in which the dominant negative Rac2-D57N mutant protein is expressed only in neutrophils, inhibiting their recruitment and rendering this fish line more susceptible to several infections (38–40). Using this genetic strategy for inhibition of neutrophil recruitment, we found that neutrophil recruitment itself is required for resistance to

mucosal candidiasis in the swim bladder (Fig. 1F). Together, these data place neutrophil recruitment and activity at the infection site as central players in protection against very early events of disease progression.

Both reduced and enhanced neutrophil recruitment impact disease progression. The commensal nature of *C. albicans* on mucosal surfaces implies that effective mechanisms are in place to protect against the development of mucosal candidiasis in the absence of damaging inflammation. Although neutrophils clearly limit mortality from mucosal candidiasis in the juvenile zebrafish model, this is a crude measure of virulence. One advantage of this model lies in its transparency and the consequent ability to track infection over time by repeated noninvasive imaging of individual animals. We exploited this to analyze the consequences of either blocking or enhancing neutrophil activity in the swim bladder. To characterize infection dynamics in the context of neutrophil inhibition, we analyzed the individual time tracks of *mpo*:*Rac2-D57N* fish compared to their wild-type (WT) siblings. To qualify progression, we categorized the infection intensity at 24-h intervals (for 72 hpi) as one of five statuses represented in Fig. 2A: low (less than 20 filaments in the swim bladder), medium (20 to 50 filaments), high (more than 50 filaments), high plus breach (more than 50 filaments with the filaments breaching the epithelial barrier), and death. These categories match well the results of quantification of the fungal burden by numbers of pixels in microscopic images (Fig. S4). The *mpo*:*Rac2-D57N* animals were not able to control the infection, with 28% of the animals progressing rapidly from a low (15 to 30 yeast cells in inoculum) to a high-plus-breach status within the first 24 hpi (Fig. 2B). For comparison, although PI3K inhibition significantly reduced neutrophil recruitment, it did not provoke significantly more breaching events at 24 hpi (Fig. S1D). This is consistent with the relatively mild exacerbation of disease progression caused by PI3K inhibition (Fig. 1D). Images of representative *mpo*:*Rac2-D57N* animals at 24 hpi clearly showed the intense invasion of surrounding tissue by filaments (Fig. 2C). By time tracking of individuals, we showed that the disease trajectories for *mpo*:*Rac2-D57N* and WT siblings were different and that the infection progressed rapidly in neutrophil recruitment-deficient animals (Fig. 2D). By 72 hpi, the majority of the *mpo*:*Rac2-D57N* animals were dead (87%), whereas only 8% of the WT siblings succumbed (Fig. 2E). This shows how the infection trajectory is altered by the defect in neutrophil recruitment, transforming a largely self-limiting and nonlethal colonization into a lethal infection. It is also important to note that neutrophil activity is a separate determinant of immunity to mucosal candidiasis, given that CXCR2 inhibition leads to increased susceptibility (Fig. 1C) and epithelial invasion (Fig. S1E) without a decrease in neutrophil recruitment (Fig. S1B and C).

The acute need for neutrophils demonstrated by longitudinal imaging suggests that enhancing early neutrophil recruitment might limit early infection progression. We investigated the impact of recruiting more neutrophils to the site of infection by coinjecting the chemoattractant leukotriene B4 (LTB4) together with *C. albicans*. LTB4 has previously been shown to recruit phagocytes to the larval zebrafish hindbrain (41). This led to a 50% increase in the number of neutrophils recruited by 24 hpi (Fig. 2F and G). Since very few breaching events occurred in immunocompetent (WT) zebrafish infected with a low inoculum, we evaluated the impact of this supernumerary recruitment by quantitatively measuring changes in the burden of *C. albicans* noninvasively in individual fish (Fig. 2H). The artificial recruitment of neutrophils to the swim bladder resulted in a nearly 25% decrease of the *C. albicans* burden compared to that in the vehicle-coinfected group (Fig. 2I).

Due to the severe defect in neutrophil migration in the *mpo*:*Rac2-D57N* fish line, it is unlikely that the strategy of chemoattractant injection would rescue the susceptibility of these fish. As an alternative approach to increase early neutrophil involvement in this fish line, we adapted current xenograft protocols (42, 43) and performed adoptive cell transfer of primary murine neutrophils into the swim bladder of zebrafish. We sorted mouse neutrophils, fluorescently labeled them, and coinjected them with *C. albicans* in the swim bladder of *mpo*:*Rac2-D57N* fish (Fig. S5A and B). The proportion of fish with

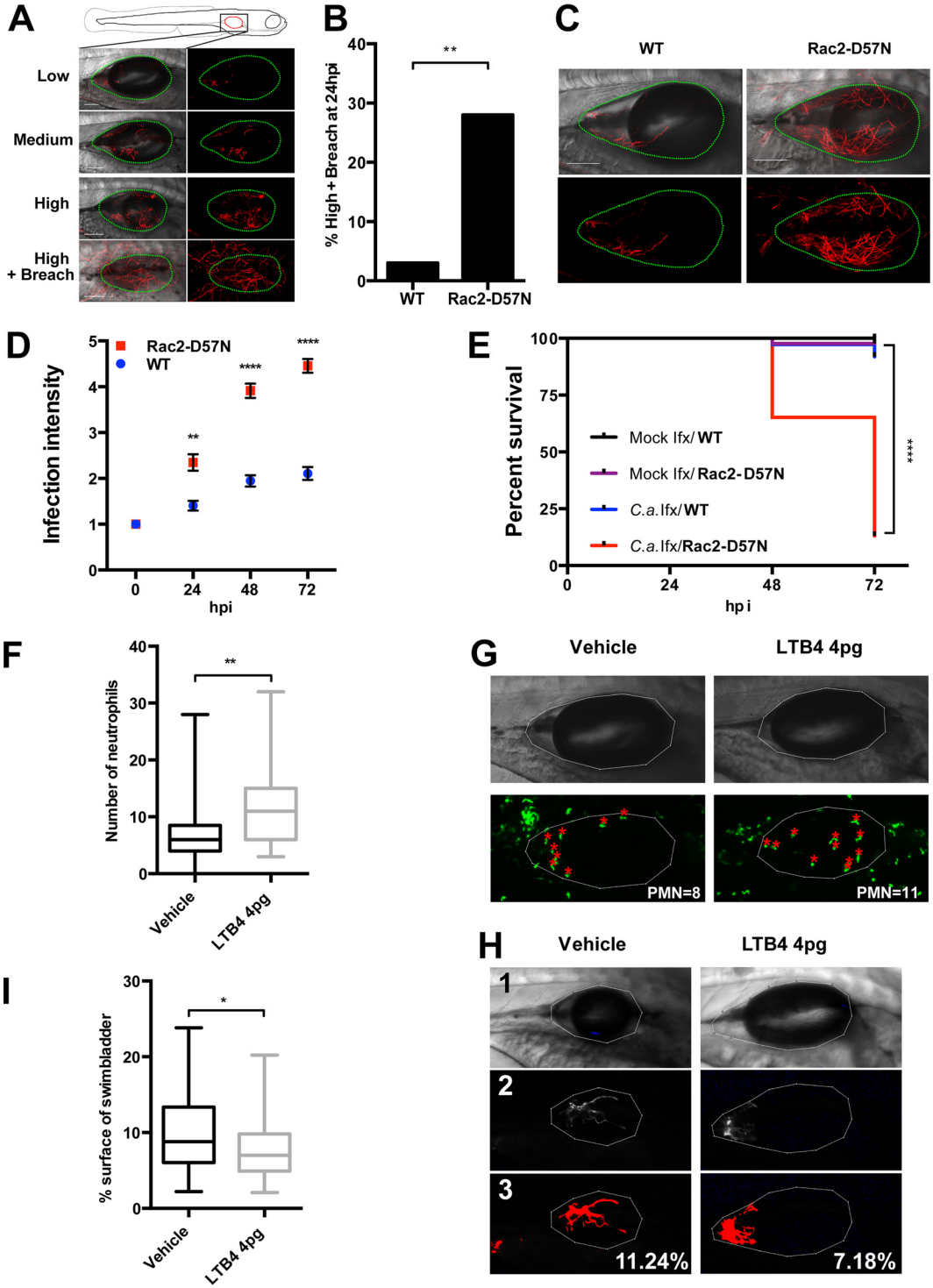

FIG 2 Up- or downmodulation of neutrophil recruitment impacts disease progression. At 4 dpf, *mpo*:*Rac2-D57N* and WT sibling (A to E) or *mpx*:*GFP* (F to I) larvae were injected into the swim bladder with 4 nl of Caf2-dTom yeast cells (10^7 CFU/ml in 5% PVP) or with PVP only. Fish were immediately screened, and only fish with 15 to 30 yeast cells were selected. Fish were imaged by confocal microscopy at 24 hpi (A to C) and at 2 and 3 days postinfection (D). (A to D) Blockade of neutrophil recruitment accelerates disease progression. (A) Representative images of the different infection levels (low, less than 20 filaments; medium, 20 to 50 filaments; high, over 50 filaments; and high plus breach, high infection level with filaments breaching the epithelial barrier). The swim bladder is outlined with green dots. Images are maximum projections in the red channel overlaid with a single slice in differential interference contrast. Bars, 100 μm. (B) Percentage of fish with high-plus-breach status at 24 hpi. Pooled percentages and the results of the Fisher exact test are represented ($P = 0.0024$). (C) Representative images of *mpo*:*Rac2-D57N* and WT fish at 24 hpi, as described in the legend to panel A. (D) Fish were longitudinally followed and scored for pathology (on a scale of 1 to 5) as described in Materials and Methods. Infection dynamics are represented by the average pathology score (mean and SEM), and the differences between infected WT and *mpo*:*Rac2-D57N* fish were analyzed by the

(Continued on next page)

a high-plus-breach status of infection at 24 hpi was decreased by almost 50% after adoptive cell transfer (Fig. S5C). However, due to the small cohort sizes in these technically challenging experiments, this did not reach statistical significance ($P = 0.14$), nor did the differences in the *C. albicans* burden at 24 hpi (Fig. S5D). Despite the lack of a robust and statistically significant difference in infection level upon adoptive transfer, these trends toward a lower level of infection are not inconsistent with the data suggesting that the recruitment of more neutrophils to the site of infection reduces the disease pressure of *C. albicans*.

Taken together, the results of these complementary experiments demonstrate quantitatively that a neutrophil presence at the site of infection impacts disease by slowing the progression of the infection. On the one hand, limited recruitment in *mpo*:*Rac2-D57N* fish speeds progression, and on the other hand, an artificially enhanced neutrophil presence slows progression.

Longitudinal tracking shows that *C. albicans* invasion of the epithelial barrier precedes death. Our data show that neutrophils can control the development of the infection but leave open the question of how they mediate protection. A role of *C. albicans* filamentation in invasion and damage has been demonstrated using epithelial layers *in vitro*, and given the high numbers of invading filaments in some fish, we reasoned that filament-mediated damage might drive overall mortality (21). Ascribing a similar role *in vivo* in a mammalian host is particularly difficult, mostly due to the technical complications in following disease progression and host-pathogen dynamics. To test the link between invasive filaments and mortality, we retrospectively analyzed the infection status of *mpo*:*Rac2-D57N* zebrafish at 48 hpi to determine their status 24 h earlier (i.e., at 24 hpi). As expected, we found that the vast majority of fish (75%) had a high-plus-breach status prior to death (Fig. 3A). Since inhibition of neutrophils leads to rapid progression of the disease in this fish line, 19% of the fish with a high infection level were dead within 24 h; these fish most probably progressed so quickly from the high status through the high-plus-breach status to death that the temporal resolution of our protocol did not allow us to catch this intermediate phase. Conversely, the clear majority of fish alive at 48 hpi had a low-burden status at 24 hpi, and very few fish (11%) with a high or a high-plus-breach status survived for 24 h (Fig. 3B). When we analyzed these data by correlating the level of infection at 24 hpi to the rate of survival at 48 hpi (Fig. 3C), we could accurately predict this relationship. Thus, in this model the early burden is closely linked to the survival time and can be used to predict the time of death.

Since we observed only filaments and not yeast breaching the epithelial barrier, we predicted that enhancing hyphal growth would increase epithelial invasion. We used the tetracycline-regulated hyperfilamentous strain tet-UME6 and its control, tet-T21, to test this idea. In the tet-UME6 strain, an overexpressed additional allele of the *UME6* gene drives hyperfilamentous growth (44). Injecting a low inoculum dose (15 to 30 yeast cells per fish) of tet-T21 or tet-UME6 led to no breaching in the tet-T21-infected fish, but 18% (7/39) of the fish injected with tet-UME6 had filaments breaching the

FIG 2 Legend (Continued)
Mann-Whitney test ($P = 0.002$, 24 hpi; $P < 0.0001$, 48 hpi; $P < 0.0001$, 72 hpi). (E) Survival curve of mock- or Caf2-dTom-infected fish over 72 hpi. In panels B, D, and E, data from three independent experiments were pooled ($n = 43$, 43, 37, and 46 for the four groups indicated from top to bottom, respectively, in the key to panel E). Data were analyzed for statistically significant differences by log-rank (Mantel-Cox) tests ($P < 0.0001$). (F to I) Artificial neutrophil recruitment reduces disease progression. *mpx*:*GFP* fish were coinjected with Caf2-dTom and 4 pg of LTB4 or vehicle. The number of neutrophils in the swim bladder at 24 hpi was counted by confocal microscopy. (F) Number of neutrophils recruited to the swim bladder at 24 hpi. (G) Representative images of infected fish with enhanced green fluorescent protein (EGFP)-expressing neutrophils in the swim bladder lumen (red asterisks) and outline of the swim bladder (in white). PMN, polymorphonuclear leukocytes. (H) Representative images of infected fish to illustrate the process used for quantification of fungal burden. Panels 1, outline of the swim bladder; panels 2, thresholding of *C. albicans*; panels 3, measurement of the percentage of the swim bladder surface covered by fungal cells. (I) *C. albicans* burden at 24 hpi by surface coverage of the swim bladder. Data were analyzed with ImageJ software. For panels F to I, data from three independent experiments were pooled ($n = 33$ and 39 for the vehicle-treated and 4 pg LTB4-treated fish, respectively). Medians, boxes, and whiskers showing the minimum-maximum are represented, and the results were tested for statistically significant differences by the Mann-Whitney test ($P = 0.001$ and $P = 0.0362$ in panels F and I, respectively). *, $P < 0.05$; **, $P < 0.01$; ***, $P < 0.001$; ****, $P < 0.0001$.

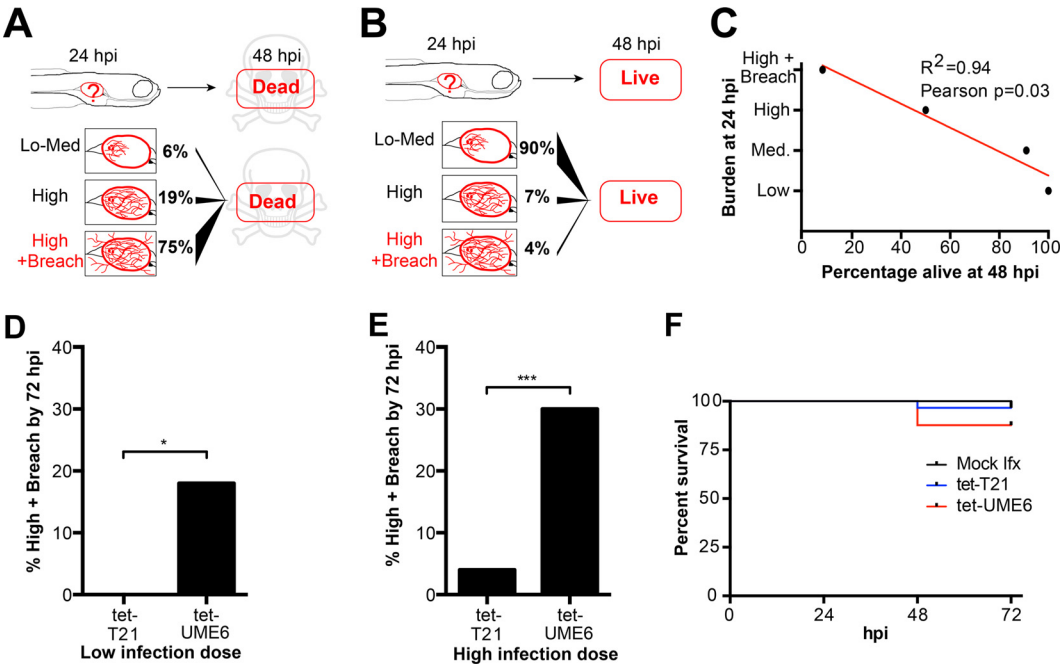

FIG 3 *Candida* filaments breach the tissue barrier, leading to death. At 4 dpf, AB and *mpo:Rac2-D57N* zebrafish were injected in the swim bladder with 4 nl of Caf2-dTom (A and B) (the data are the same as those used for Fig. 2A to E) or 10^7 CFU/ml (C) and 3×10^7 CFU/ml (D and E) of tet-T21-dTomato (tet-T21) or tet-UME6-dTomato (tet-UME6). The fish were immediately screened, and only fish with 15 to 30 (C) or 50 to 100 (D and E) yeast cells were selected. Fish were imaged by confocal microscopy every 24 h for 3 days. (A to C) Death is due to filament breaching of the epithelial barrier. (A and B) Diagrams representing the findings of the retrospective analysis of the burden status at 24 hpi of fish dead (A) or alive (B) at 48 hpi. (C) Average percentage of fish alive at 48 hpi from each infection level at 24 hpi. The regression line (red), the R^2 value, and the *P* value obtained by the Pearson correlation test are shown. Data from three independent experiments were pooled (the data are the same as those used for Fig. 2A to E). (D to F) Active filamentation is involved in breaching of the epithelial barrier. (D and E) Percentage of fish receiving a low infection dose (D) and a high infection dose (E) with barrier breach by filaments (high-plus-breach status) after 72 h of infection with tet-T21 and tet-UME6. Data from three independent experiments were pooled (for the low infection dose, $n = 35$ and 39 tet-T21 and tet-UME6 fish, respectively; for the high infection dose, $n = 56$ and 53 tet-T21 and tet-UME6 fish, respectively); the differences in the overall percentages were evaluated by Fisher's exact test ($P = 0.0123$ and $P = 0.0002$ in panels D and E, respectively). (F) The survival of fish injected with PVP, tet-T21, and tet-UME6 (50 to 100 yeast cells) over 72 h is represented (Kaplan-Meier test). Data from three independent experiments were pooled ($n =$ 56, 56, and 53 for mock-infected fish and fish infected with tet-T21 and tet-UME6, respectively). *, $P < 0.05$; ***, $P < 0.001$.

epithelium by 72 hpi (Fig. 3D). When a high inoculum dose (50 to 100 yeast cells per fish) was used, 4% (2/56) of the fish into which tet-T21 was injected and 30% (16/53) of the fish into which tet-UME6 was injected had a breach of the epithelial barrier (Fig. 3E). Since these experiments were conducted in immunocompetent fish, the associated mortality was low in this time frame, but more fish succumbed to the infection with tet-UME6 than to the infection with tet-T21 at both infection doses (Fig. 3F and data not shown).

These data demonstrate that the breaching of the epithelial barrier, which in the juvenile zebrafish model leads to death, is an intrinsic property of *C. albicans* filaments. Taken together with our results that suggest a key role for neutrophils in controlling the infection, we reasoned that neutrophils must play an important role in limiting filamentous invasion. However, our data did not suggest a mechanism whereby neutrophils might prevent *C. albicans* invasion of the epithelial barrier.

The levels of extracellular DNA and *C. albicans* damage depend on the presence of neutrophils at the site of infection. Neutrophils produce inhibitory extracellular traps (ETs) *in vitro*, preferentially in response to *C. albicans* filaments that are targeted through frustrated phagocytosis (45). To evaluate the elaboration of ETs against *C. albicans* at the mucosal surface, we used *in vivo* staining with the membrane-impermeant Sytox green dye. This dye labels extracellular DNA and can also enter damaged *C. albicans* filaments. We injected the swim bladder of infected *mpo:Rac2-D57N* and WT sibling fish with Sytox green at 20 hpi and performed two-dimensional

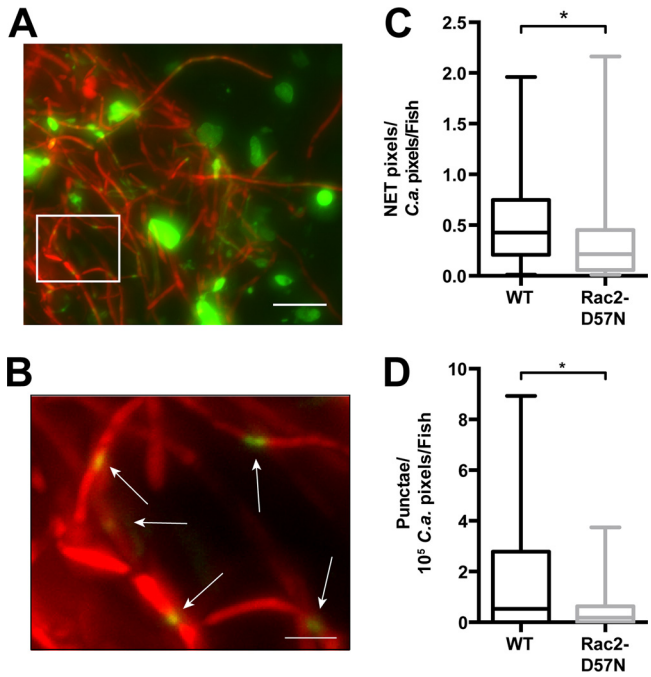

FIG 4 Blockade of neutrophil recruitment reduces both extracellular DNA levels and the extent of damaged *C. albicans*. At 4 dpf, *mpo*:*Rac2-D57N* and WT sibling zebrafish were injected in the swim bladder with 4 nl of Caf2-dTom (10^7 CFU/ml) or PVP. The fish were immediately screened, and only fish with 15 to 30 yeast cells in the swim bladder were selected. Fish were injected at 20 hpi with 2 nl of Sytox green (0.05 mM) and imaged by epifluorescence microscopy 4 h later. Each image was analyzed with ImageJ software as described in Materials and Methods for determination of the amount of *C. albicans* (number of pixels in the red channel) and extracellular DNA (number of pixels in the green channel). The number of punctae on filaments was also scored. Both the number of pixels (extracellular DNA) and the number of punctae (*C. albicans* damage) were normalized to the amount of *C. albicans* (number of pixels) in each image resulting in the ET/*C. albicans* ratio indicated in panel C or the ratio of the number of punctae/10^5 pixels of *C. albicans* indicated in panel D. (A and B) Representative image of 2D staining for extracellular DNA and *C. albicans* damage. Images were processed by overlaying the projection of the sum of slices in both the red and green channels. (B) Zoomed image of the box in panel A, with white arrows pointing to punctae (green) on *C. albicans* filaments (red). Bars, 20 μm (A) and 5 μm (B). (C) Loss of neutrophil recruitment in the *mpo*:*Rac2-D57N* line decreases the amount of extracellular DNA. The ratio of green pixels (extracellular DNA) to total red pixels (*C. albicans*) was calculated using ImageJ software, and the average ratio per fish is shown for *mpo*:*Rac2-D57N* and WT siblings. Data from three independent experiments were pooled ($n = 27$ and 30 for *mpo*:*Rac2-D57N* and WT fish, respectively). Medians, boxes, and whiskers showing the minimum-maximum are represented with the results of the Mann-Whitney test ($P = 0.0295$). (D) Loss of neutrophil recruitment in the *mpo*:*Rac2-D57N* line decreases *C. albicans* damage. The number of punctae on each image was normalized to the amount of *C. albicans*, and the average ratio per fish for fish with WT Rac2 and Rac2-D57N neutrophils is shown. Data from three independent experiments were pooled ($n = 27$ and 30 for *mpo*:*Rac2-D57N* and WT fish, respectively). Medians, boxes, and whiskers showing the minimum-maximum are represented with the results of the Mann-Whitney test ($P = 0.0201$). *, $P < 0.05$.

(2D) imaging 4 h later (24 hpi). The images were then quantified for both the area covered by extracellular DNA and the number of *C. albicans* filaments with green punctae (Fig. 4A and B). Quantification of ETs by percent coverage of microscopy fields is standard in the field due to the difficulty in assigning ET structures to individual neutrophils (17, 45). The method of processing of the ET images was similar to that performed in the experiment whose results are presented in Fig. 2H, where fluorescence images were thresholded and the number of fluorescent pixels in each channel was quantified. The *mpo*:*Rac2-D57N* fish, which are more susceptible to mucosal candidiasis and lack neutrophilic infiltration to the swim bladder lumen, had significantly less extracellular DNA (33%) than their WT siblings (Fig. 4C). This suggests that neutrophil infiltration is required for full ET production. Residual extracellular DNA in the absence of recruited neutrophils may arise from macrophage ETs, which are weakly cytotoxic and produced *in vitro* in response to *C. albicans* (46). We do not rule out the

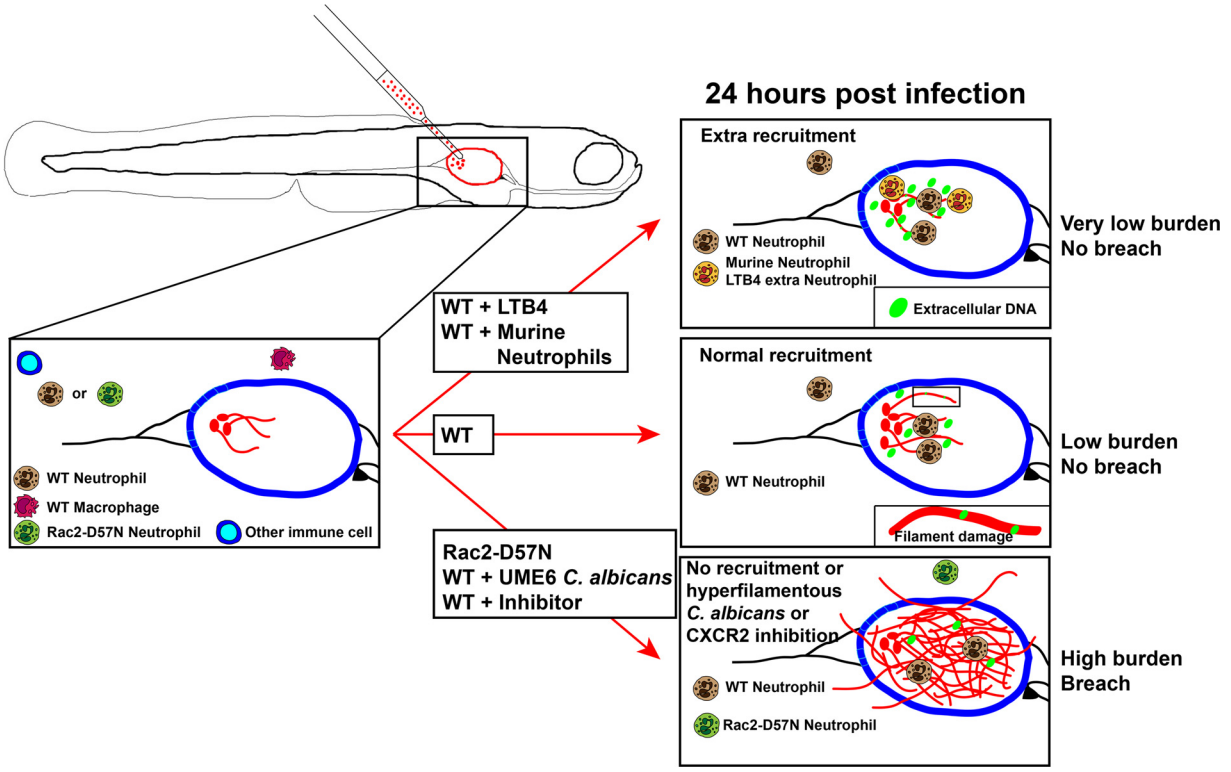

FIG 5 Summary diagram. In immunocompetent wild-type (WT) fish, neutrophils are rapidly recruited to the site of infection, extracellular DNA is present, and hyphal filaments are damaged by 24 hpi, leading to control of the infection. No mortality occurs within the first 3 days postinfection, and disease progression is slow. In immunocompromised animals or if hypervirulent *C. albicans* is injected (bottom arrow), neutrophils are not able to control the infection and filaments breach the epithelial barrier and invade the surrounding tissues. This leads to rapid mortality. Conversely, if extra neutrophils are recruited to the site of infection shortly after infection (top arrow), the infection is contained more efficiently.

possible protective role of macrophage ETs against *C. albicans* hyphae, but the redundancy of macrophages in our model argues against this idea (Fig. 1E). Remarkably, *mpo*:*Rac2D57N* fish with defective neutrophils had 4-fold fewer damaged *C. albicans* filament segments than their immunocompetent siblings (Fig. 4D). This suggests that neutrophils are required to damage hyphae at the mucosal epithelium.

DISCUSSION

Mucosal candidiasis is a common disease, but we are only beginning to understand the roles of neutrophils in the prevention and exacerbation of disease. The dual nature of neutrophils in candidiasis is highlighted by the paradox that neutrophils protect against mucosal-blood dissemination but exacerbate symptoms in human *C. albicans* vaginitis (4). The larval zebrafish swim bladder represents a tremendous opportunity for modeling mucosal disease dynamics and understanding neutrophil activities at the mucosal surface, enabling noninvasive, high-resolution tracking of disease progression. Using this model, we found that neutrophils protect against candidiasis in the swim bladder mucosa, where they prevent epithelial invasion by filaments and maintain *C. albicans* as a colonizer rather than a pathogen (Fig. 5). Intriguingly, our longitudinal imaging suggests that neutrophils in the mucosal lumen damage hyphae with extracellular traps and prevent their invasion of epithelia. These findings offer important mechanistic clues about the reason why neutrophils are so important in protection against oral candidiasis.

Our findings establish the juvenile zebrafish swim bladder model as a versatile and unique tool for exploring the dynamics of mucosal infections and the vertebrate innate immune system. Several technical advantages of the larval zebrafish model were instrumental in providing new insight into neutrophilic control of mucosal candidiasis. The translucency and small size of zebrafish, coupled with the availability of fluorescent

transgenic lines, enabled quantitative longitudinal imaging of disease in the context of neutrophil recruitment perturbations. This powerful high-content imaging approach to understanding pathogenesis is likely to be of great use, especially for probing the genetic basis of localized infection dynamics in the context of both phagocytic innate immune cells and the epithelium.

Protection from mucosal candidiasis in the juvenile zebrafish involves neutrophil recruitment and activation through conserved signaling pathways, demonstrating the relevance of this model for the study of *C. albicans* pathogenesis. Rac2, PI3K, and CXCR2 are all important in neutrophil activity in both zebrafish and mammals (34, 38, 47–50). Further, the unchanged neutrophil recruitment upon CXCR2 inhibition suggests that neutrophil activation may be an important function of CXCR2. A variety of studies in mouse and zebrafish suggest that CXCR2 plays a complex time- and organ-specific role in neutrophil recruitment (47, 48, 51, 52). A potential role of CXCR2 in activation is supported by studies showing that CXCR2 activates neutrophil killing by neutrophil extracellular traps (NETs) and is specifically required against *C. albicans* hyphae (47, 49). The recruitment-independent activity of chemokine receptors has also been observed in murine CXCR1 deficiency and may therefore be a widely used potentiator of efficient killing (53).

In contrast to the important role for neutrophils, macrophages play a redundant role in defense in the swim bladder. We showed this using selective, conditional ablation of nitroreductase-expressing macrophages. This is the first time that this strategy has been used to evaluate the functional role of macrophages in protection against mucosal candidiasis. Our results are consistent with those of previous work that suggest that macrophages have a relatively minor role in protection against mucosal candidiasis (46, 54, 55). Although macrophages are efficient at yeast phagocytosis and can contain germination *in vivo* (36), neutrophil attack of any extra hyphae arising from nonphagocytosed fungi may be sufficient to protect against epithelial invasion.

Our data suggest that neutrophil numbers and activation are of high importance in reducing the fungal burden and stopping invasion. The strategies that we used to come to these conclusions (longitudinal imaging and neutrophil modulation) have not yet been applied to this question and therefore add weight to the hypothesis that neutrophil recruitment and/or activation at the site of infection controls the progression of disease. This is consistent with several studies of murine oral candidiasis but is in contrast to the findings of studies of vulvovaginal candidiasis that suggested that neutrophil recruitment is detrimental rather than protective (4). Our data also show that blockade of neutrophil recruitment results in an increased pathogen load and less damage to fungal hyphae, suggesting that neutrophils protect by damaging fungi rather than promoting disease tolerance (56). This leaves open the questions of exactly how *C. albicans* manages to invade and how neutrophils manage to control invasion of the epithelium.

From the fungal perspective, our data bring together and validate the *in vivo* relevance of the findings of a series of *in vitro* studies that clearly implicate hyphae as a major contributor to endocytosis, invasion, and epithelial damage (22, 57). Using the zebrafish model to integrate the concept of filament-mediated invasion into the context of mucosal immunity, we demonstrated a requirement of neutrophil activity for limiting fungal hyphal growth and invasion. Interestingly, the filament-locked tet-UME6 strain is hyperinvasive, suggesting that invasion is an intrinsic characteristic of filaments rather than being dependent on active dimorphic switching or the combined activity of filaments and yeast. Creation of novel transgenic zebrafish lines may allow a more detailed molecular dissection of these invasion events to determine if penetration is transcellular, paracellular, or dependent on epithelial damage (55).

From the host perspective, our quantitative three-dimensional imaging of the infection site suggests that extracellular traps (ETs) play a key role in damaging filaments and limiting invasion. ETs are present in mucosal *C. albicans* infections in mice, but to date no correlation of neutrophil activity with ETs and fungal damage *per se* has been explored in murine models (12, 17). Our observations link mucosal ET

production to neutrophil recruitment and, further, show a correlation between neutrophil-dependent ET production and higher levels of fungal damage, although it remains to be demonstrated that ETs directly damage *C. albicans* filaments *in vivo*. This is consistent with recent observations that suggest that NETs are required to damage *C. albicans* filaments during disseminated candidiasis (58).

Our findings in the zebrafish model of mucosal candidiasis show that neutrophils are essential for protection against hyphal invasion of the epithelial layer and suggest that this involves the production of ETs. These data demonstrate that there are conserved innate immune mechanisms for containing commensal *C. albicans* between the zebrafish swim bladder and the mouse oral cavity, establishing the larval swim bladder as a potential tool for understanding longitudinal host-pathogen interactions in the oral mucosa and testing potential therapeutics. Finally, the model used here can contribute significantly to unraveling the mechanisms of neutrophil recruitment dynamics, NET formation, modes of *C. albicans* damage, and mechanisms of *C. albicans* epithelial invasion *in vivo*.

MATERIALS AND METHODS

Animal care and maintenance. All zebrafish were kept in recirculating systems (Aquatic Habitats) at the University of Maine Zebrafish Facility under a 14-h light/10-h dark cycle. The water temperature was kept at 28°C. Collected eggs were reared to 4 days postfertilization (dpf) at 33°C as described previously (28). The fish lines used were wild-type (WT) AB from ZIRC, *Tg*(*BACmpo*:*gfp*)^{114} as described previously (59) and referred to here as *mpx*:*GFP*, *Tg*(*mpo*:*mCherry-A2-Rac2D57N*) as described previously (38) and referred to here as *mpo*:*Rac2-D57N*, as well as *mpeg1*:*Gal4* (60) crossed with *UAS*:*NfsB-mCherry* (52) and referred to here as *mpeg1-NTR* and *mpeg1*:*EGFP* (60). When the *mpo*:*Rac2-D57N* line was used, heterozygous transgenic females were crossed with AB males and the progeny were sorted for the presence of mCherry neutrophils (Rac2-D57N) or their absence (WT siblings). (See https://wiki.zfin.org/display/general/ZFIN+Zebrafish+Nomenclature+Guidelines for the genetic nomenclature for zebrafish.) All zebrafish care and husbandry procedures were performed as described previously (61). Mice were maintained at the Small Animal Research Facility at the University of Maine. Female C57BL/6J mice (The Jackson Laboratory) were used at 6 to 12 weeks of age for bone marrow neutrophil isolation.

Ethics statement. All zebrafish studies were carried out in accordance with the recommendations in the *Guide for the Care and Use of Laboratory Animals* of the National Research Council (62). All animals were treated in a humane manner according to the guidelines of the University of Maine IACUC, as detailed in protocol number A2015-11-03. The University of Maine IACUC/Ethics Committee approved this protocol. Animals were euthanized by tricaine overdose. Infected animals were monitored daily for signs of infection, and morbid animals were euthanized. All mouse studies were carried out in accordance with the recommendations in the *Guide for the Care and Use of Laboratory Animals* (62). All animals were treated in a humane manner according to the guidelines of the University of Maine IACUC, as detailed in protocol number A2014-02-01. The University of Maine IACUC/Ethics Committee approved this protocol. Animals were euthanized by carbon dioxide inhalation.

Fungal strains and growth conditions. The *C. albicans* Caf2-dTomato (Caf2-dTom) strain (33) was grown on yeast-peptone-dextrose (YPD) agar. For infections, liquid cultures of *C. albicans* were grown overnight in YPD at 30°C on a roller drum (New Brunswick Scientific). For creation of fluorescent protein-expressing strains, tetracycline-regulated strains TT21 and TUME6 (34) were plated on YPD agar containing 50 μg/ml of doxycycline (Dox) and transformed with the pENO1-dTom-NATr plasmid as described previously (33). The resulting genotypes are as follows: for strain tet-T21, *ade2*::*hisG/ade2*::*hisG ura3*::*imm434/ura3*::*imm434*::*URA3-tetO ENO1/ENO1*::*ENO1-dTomato-NatR-ENO1-tetR-ScHAP4AD-3XHA-ADE2*, and for strain tet-UME6, *ade2*::*hisG/ade2*::*hisG ura3*::*imm434/ura3*::*imm434*::*URA3-tetO-UME6 ENO1/ENO1*::*ENO1-tetR-ScHAP4AD-3XHA-ADE2-ENO1-dTomato-NatR*. Integration was confirmed by diagnostic PCR using primers SP6 (5′-GATTTAGGTGACACTATAG-3′) and dTomato Rv2 (5′-AAGGTCTACCTTCACCTTCACC-3′) for tet-UME6 or Peno1-genomic F1 (5′-TCCTTGGCTGGCACTGAACTCG-3′) and dTomato Rv2 for tet-T21. For infection, liquid cultures of tet-T21 and tet-UME6 were grown overnight in YPD-Dox (50 μg/ml) at 30°C on a roller drum. Overnight cultures were washed twice in phosphate-buffered saline (PBS) and resuspended to the appropriate concentration in 5% polyvinylpyrrolidone (PVP).

Bacterial strains and growth conditions. *Pseudomonas aeruginosa* PA14-dTomato (63) was plated on LB agar with ampicillin (Amp; 750 μg/ml) and incubated at 37°C overnight. A single colony was picked, inoculated in 2 ml of LB with 750 μg/ml Amp, and incubated on a roller drum at 37°C overnight. One milliliter of the culture was washed twice with 1 ml of PBS, and the optical density at 600 nm (OD_{600}) was measured against a PBS blank. The bacterial concentration, based on a conversion in which an OD_{600} of 1 is equivalent to 10^9/ml, was adjusted to 10^9 CFU/ml in 5% PVP before injection.

Chemical treatment. Fish were incubated in 6-well plates with 10 ml of E3 plus 1-phenyl-2-thiourea (PTU; 10 μg/ml) containing SB225002 (2 μg/ml), LY294002 (5 μg/ml), or the relevant concentration of vehicle (dimethyl sulfoxide [DMSO]) for 1 h prior to injection. The fish were then anesthetized and injected as described below, screened by microscopy for proper inoculum injection, and returned to 6-well plates with E3 containing the same chemicals. The medium was changed daily, and mortality was recorded. Metronidazole ablation was done as described previously (37). For coinjection of leukotriene

B4 (LTB4; Cayman Chemicals), the Caf2-dTom strain was diluted to 10^7 CFU/ml in 5% PVP containing 1 μg/ml of LTB4.

Microinjection. At 4 dpf, larvae reared at 33°C were screened for an inflated swim bladder and injected in the swim bladder with 4 nl of *Candida albicans* in PVP or PVP only as described previously (28). For ear injection, at 3 dpf larvae reared at 33°C were injected in the otic vesicle with 1 nl of *Candida albicans* (2×10^7 CFU/ml) or *Pseudomonas aeruginosa* (10^9 CFU/ml) in 5% PVP or PVP only. The fish were then returned to E3 plus PTU in a 33°C incubator or 35°C for the adoptive cell transfer experiments. For extracellular DNA and filament damage experiments, at 5 dpf fish were similarly anesthetized and injected in the swim bladder with 2 nl of Sytox green (0.05 mM) or 5% DMSO.

Adoptive cell transfer. Murine neutrophils were purified from bone marrow as described previously (58, 64). After collection and enumeration, neutrophils were diluted to 2.5×10^7 cells/ml in sterile Hanks' buffered saline solution (HBSS; Gibco) with 10% fetal calf serum (FCS; Lonza). Cells were spun down (1,000 rpm for 5 min), resuspended in 5 ml carboxyfluorescein succinimidyl ester (2 μM in HBSS; Invitrogen), and incubated on ice in the dark for 8 min. The reaction was stopped by adding 7 ml of HBSS plus 20% FCS. The cells were then enumerated, spun down, and resuspended to 10^7 cells/ml in HBSS plus 5% PVP with or without Caf2-dTom at 10^7 CFU/ml.

Fluorescence microscopy. For live imaging, fish were imaged as described previously (33) using a 96-well glass-bottom imaging dish (Greiner-Bio). Confocal imaging was carried out using an Olympus IX-81 inverted microscope with an FV-1000 laser scanning confocal system (Olympus). A 20× objective lens (numerical aperture [NA], 0.7; Olympus) was used. Enhanced green fluorescent protein (EGFP) or Sytox green and dTomato (dTom) fluorescent proteins were detected by the use of laser and optical filters of 488 nm excitation/510 nm emission and 543 nm excitation/618 nm emission, respectively. Images were collected with a FluoView microscope (Olympus) and processed using a Fiji plug-in (ImageJ environment) (65). For 2D imaging of filaments and extracellular DNA, fish were euthanized and individually placed on a glass slide (25 by 75 mm; Corning). A glass coverslip (12 by 12 mm; catalog number 1.5; VWR) was placed on top of the fish and pressed down using the bulb of a plastic Pasteur pipette to gently flatten the euthanized fish. Images were acquired on a Zeiss AxioVision Vivatome microscope (Zeiss) using a 40× objective (NA, 0.75; Zeiss) and processed using the Fiji plug-in (NIH) as detailed in the Materials and Methods in the supplemental material. To estimate the *C. albicans* burden by direct visualization under an epifluorescence microscope, pathology was scored as low for less than 20 filaments in the swim bladder, medium for 20 to 50 filaments, high for more than 50 filaments, high plus breach for more than 50 filaments accompanied by epithelial invasion by *C. albicans*, and dead for dead fish. Representative images of the pathology receiving each score are shown in Fig. 2A. To compare the infection pathology between groups in Fig. 2D, infection categories were assigned numbers, and the average pathology score was calculated (where a low pathology score was given a value of 1, a medium score was given a value of 2, a high score was given a value of 3, a high plus breach score was given a value of 4, and dead was given a value of 5). The number of neutrophils or macrophages recruited to the swim bladder was recorded only for fish with no filaments breaching the epithelial barrier.

Statistics. Prism software (version 6; GraphPad Software Inc.) was used for analysis of the statistics. Survival data were analyzed by the Kaplan-Meier method with Mantel-Cox log-rank testing. Other data were analyzed by nonparametric tests throughout (the Kruskal-Wallis test with Dunn's multiple-comparison test for more than two groups or the Mann-Whitney test for two groups), as detailed in the figure legends. *P* values were considered significant when *P* was <0.05, <0.01, <0.001, and <0.0001, as indicated in the figure legends. Within the limits of the statistical tests calculated in Prism software (version 6), exact *P* values are included in the figure legends.

SUPPLEMENTAL MATERIAL

Supplemental material for this article may be found at https://doi.org/10.1128/IAI.00276-17.

SUPPLEMENTAL FILE 1, PDF file, 1.4 MB.

ACKNOWLEDGMENTS

We thank Anna Huttenlocher (University of Wisconsin) for a fish line (the *mpo:Rac2-D57N* line) and Brian Peters (University of Tennessee Health Science Center) for the *C. albicans* strains (TUME6 and TT21). We acknowledge Alex Hopke for technical advice on murine neutrophil isolation, Mark Nilan for superior fish care, and members of the R. T. Wheeler lab for stimulating discussions.

This work was supported by NIH grant R15AI094406 and USDA Hatch grant number ME0-H-1-00517-13 to R.T.W. R.T.W. is a PATH investigator of the Burroughs Wellcome Fund.

REFERENCES

1. Brown GD, Denning DW, Gow NA, Levitz SM, Netea MG, White TC. 2012. Hidden killers: human fungal infections. Sci Transl Med 4:165rv13. https://doi.org/10.1126/scitranslmed.3004404.

2. Enoch DA, Ludlam HA, Brown NM. 2006. Invasive fungal infections: a review of epidemiology and management options. J Med Microbiol 55:809–818. https://doi.org/10.1099/jmm.0.46548-0.

3. Casadevall A, Pirofski LA. 2003. The damage-response framework of microbial pathogenesis. Nat Rev Microbiol 1:17–24. https://doi.org/10.1038/nrmicro732.
4. Jabra-Rizk MA, Kong EF, Tsui C, Nguyen MH, Clancy CJ, Fidel PL, Jr, Noverr M. 2016. Candida albicans pathogenesis: fitting within the host-microbe damage response framework. Infect Immun 84:2724–2739. https://doi.org/10.1128/IAI.00469-16.
5. Okada S, Puel A, Casanova JL, Kobayashi M. 2016. Chronic mucocutaneous candidiasis disease associated with inborn errors of IL-17 immunity. Clin Transl Immunol 5:e114. https://doi.org/10.1038/cti.2016.71.
6. Lortholary O, Dupont B. 1997. Antifungal prophylaxis during neutropenia and immunodeficiency. Clin Microbiol Rev 10:477–504.
7. Scully C, el-Kabir M, Samaranayake LP. 1994. Candida and oral candidosis: a review. Crit Rev Oral Biol Med 5:125–157. https://doi.org/10.1177/10454411940050020101.
8. Villar CC, Dongari-Bagtzoglou A. 2008. Immune defence mechanisms and immunoenhancement strategies in oropharyngeal candidiasis. Expert Rev Mol Med 10:e29. https://doi.org/10.1017/S1462399408000835.
9. Altmeier S, Toska A, Sparber F, Teijeira A, Halin C, LeibundGut-Landmann S. 2016. IL-1 coordinates the neutrophil response to C. albicans in the oral mucosa. PLoS Pathog 12:e1005882. https://doi.org/10.1371/journal.ppat.1005882.
10. Aratani Y, Kura F, Watanabe H, Akagawa H, Takano Y, Suzuki K, Dinauer MC, Maeda N, Koyama H. 2002. Relative contributions of myeloperoxidase and NADPH-oxidase to the early host defense against pulmonary infections with Candida albicans and Aspergillus fumigatus. Med Mycol 40:557–563.
11. Huppler AR, Conti HR, Hernandez-Santos N, Darville T, Biswas PS, Gaffen SL. 2014. Role of neutrophils in IL-17-dependent immunity to mucosal candidiasis. J Immunol 192:1745–1752. https://doi.org/10.4049/jimmunol.1302265.
12. Trautwein-Weidner K, Gladiator A, Nur S, Diethelm P, LeibundGut-Landmann S. 2015. IL-17-mediated antifungal defense in the oral mucosa is independent of neutrophils. Mucosal Immunol 8:221–231. https://doi.org/10.1038/mi.2014.57.
13. Lam S, Hsia CC. 2012. Peripheral blood candidiasis. Blood 119:4822. https://doi.org/10.1182/blood-2011-09-378737.
14. Nadir E, Kaufshtein M. 2005. Images in clinical medicine. Candida albicans in a peripheral-blood smear. N Engl J Med 353:e9.
15. Peters BM, Yano J, Noverr MC, Fidel PL, Jr. 2014. Candida vaginitis: when opportunism knocks, the host responds. PLoS Pathog 10:e1003965. https://doi.org/10.1371/journal.ppat.1003965.
16. Fidel PL, Jr, Barousse M, Espinosa T, Ficarra M, Sturtevant J, Martin DH, Quayle AJ, Dunlap K. 2004. An intravaginal live Candida challenge in humans leads to new hypotheses for the immunopathogenesis of vulvovaginal candidiasis. Infect Immun 72:2939–2946. https://doi.org/10.1128/IAI.72.5.2939-2946.2004.
17. Branzk N, Lubojemska A, Hardison SE, Wang Q, Gutierrez MG, Brown GD, Papayannopoulos V. 2014. Neutrophils sense microbe size and selectively release neutrophil extracellular traps in response to large pathogens. Nat Immunol 15:1017–1025. https://doi.org/10.1038/ni.2987.
18. Ermert D, Urban CF, Laube B, Goosmann C, Zychlinsky A, Brinkmann V. 2009. Mouse neutrophil extracellular traps in microbial infections. J Innate Immun 1:181–193. https://doi.org/10.1159/000205281.
19. Gabrielli E, Sabbatini S, Roselletti E, Kasper L, Perito S, Hube B, Cassone A, Vecchiarelli A, Pericolini E. 2016. In vivo induction of neutrophil chemotaxis by secretory aspartyl proteinases of Candida albicans. Virulence 7:819–825. https://doi.org/10.1080/21505594.2016.1184385.
20. Mayer FL, Wilson D, Hube B. 2013. Candida albicans pathogenicity mechanisms. Virulence 4:119–128. https://doi.org/10.4161/viru.22913.
21. Moyes DL, Wilson D, Richardson JP, Mogavero S, Tang SX, Wernecke J, Hofs S, Gratacap RL, Robbins J, Runglall M, Murciano C, Blagojevic M, Thavaraj S, Forster TM, Hebecker B, Kasper L, Vizcay G, Iancu SI, Kichik N, Hader A, Kurzai O, Luo T, Kruger T, Kniemeyer O, Cota E, Bader O, Wheeler RT, Gutsmann T, Hube B, Naglik JR. 2016. Candidalysin is a fungal peptide toxin critical for mucosal infection. Nature 532:64–68. https://doi.org/10.1038/nature17625.
22. Wachtler B, Citiulo F, Jablonowski N, Forster S, Dalle F, Schaller M, Wilson D, Hube B. 2012. Candida albicans-epithelial interactions: dissecting the roles of active penetration, induced endocytosis and host factors on the infection process. PLoS One 7:e36952. https://doi.org/10.1371/journal.pone.0036952.
23. Zhu W, Filler SG. 2010. Interactions of Candida albicans with epithelial cells. Cell Microbiol 12:273–282. https://doi.org/10.1111/j.1462-5822.2009.01412.x.
24. Tobin DM, May RC, Wheeler RT. 2012. Zebrafish: a see-through host and a fluorescent toolbox to probe host-pathogen interaction. PLoS Pathog 8:e1002349. https://doi.org/10.1371/journal.ppat.1002349.
25. Gratacap RL, Wheeler RT. 2014. Utilization of zebrafish for intravital study of eukaryotic pathogen-host interactions. Dev Comp Immunol 46:108–115. https://doi.org/10.1016/j.dci.2014.01.020.
26. Lieschke GJ, Currie PD. 2007. Animal models of human disease: zebrafish swim into view. Nat Rev Genet 8:353–367. https://doi.org/10.1038/nrg2091.
27. Gabor KA, Goody MF, Mowel WK, Breitbach ME, Gratacap RL, Witten PE, Kim CH. 2014. Influenza A virus infection in zebrafish recapitulates mammalian infection and sensitivity to anti-influenza drug treatment. Dis Model Mech 7:1227–1237. https://doi.org/10.1242/dmm.014746.
28. Gratacap RL, Bergeron AC, Wheeler RT. 2014. Modeling mucosal candidiasis in larval zebrafish by swimbladder injection. J Vis Exp 2014:e52182. https://doi.org/10.3791/52182.
29. Zhang Y, Liu H, Yao J, Huang Y, Qin S, Sun Z, Xu Y, Wan S, Cheng H, Li C, Zhang X, Ke Y. 2016. Manipulating the air-filled zebrafish swim bladder as a neutrophilic inflammation model for acute lung injury. Cell Death Dis 7:e2470. https://doi.org/10.1038/cddis.2016.365.
30. Cheng SC, Joosten LA, Kullberg BJ, Netea MG. 2012. Interplay between Candida albicans and the mammalian innate host defense. Infect Immun 80:1304–1313. https://doi.org/10.1128/IAI.06146-11.
31. Winata CL, Korzh S, Kondrychyn I, Zheng W, Korzh V, Gong Z. 2009. Development of zebrafish swimbladder: the requirement of Hedgehog signaling in specification and organization of the three tissue layers. Dev Biol 331:222–236. https://doi.org/10.1016/j.ydbio.2009.04.035.
32. Zheng W, Wang Z, Collins JE, Andrews RM, Stemple D, Gong Z. 2011. Comparative transcriptome analyses indicate molecular homology of zebrafish swimbladder and mammalian lung. PLoS One 6:e24019. https://doi.org/10.1371/journal.pone.0024019.
33. Gratacap RL, Rawls JF, Wheeler RT. 2013. Mucosal candidiasis elicits NF-kappaB activation, proinflammatory gene expression and localized neutrophilia in zebrafish. Dis Model Mech 6:1260–1270. https://doi.org/10.1242/dmm.012039.
34. Deng Q, Sarris M, Bennin DA, Green JM, Herbomel P, Huttenlocher A. 2013. Localized bacterial infection induces systemic activation of neutrophils through Cxcr2 signaling in zebrafish. J Leukoc Biol 93:761–769. https://doi.org/10.1189/jlb.1012534.
35. Moyes DL, Shen C, Murciano C, Runglall M, Richardson JP, Arno M, Aldecoa-Otalora E, Naglik JR. 2014. Protection against epithelial damage during Candida albicans infection is mediated by PI3K/Akt and mammalian target of rapamycin signaling. J Infect Dis 209:1816–1826. https://doi.org/10.1093/infdis/jit824.
36. Brothers KM, Gratacap RL, Barker SE, Newman ZR, Norum A, Wheeler RT. 2013. NADPH oxidase-driven phagocyte recruitment controls Candida albicans filamentous growth and prevents mortality. PLoS Pathog 9:e1003634. https://doi.org/10.1371/journal.ppat.1003634.
37. Voelz K, Gratacap RL, Wheeler RT. 2015. A zebrafish larval model reveals early tissue-specific innate immune responses to Mucor circinelloides. Dis Model Mech 8:1375–1388. https://doi.org/10.1242/dmm.019992.
38. Deng Q, Yoo SK, Cavnar PJ, Green JM, Huttenlocher A. 2011. Dual roles for Rac2 in neutrophil motility and active retention in zebrafish hematopoietic tissue. Dev Cell 21:735–745. https://doi.org/10.1016/j.devcel.2011.07.013.
39. Harvie EA, Green JM, Neely MN, Huttenlocher A. 2013. Innate immune response to Streptococcus iniae infection in zebrafish larvae. Infect Immun 81:110–121. https://doi.org/10.1128/IAI.00642-12.
40. Knox BP, Deng Q, Rood M, Eickhoff JC, Keller NP, Huttenlocher A. 2014. Distinct innate immune phagocyte responses to Aspergillus fumigatus conidia and hyphae in zebrafish larvae. Eukaryot Cell 13:1266–1277. https://doi.org/10.1128/EC.00080-14.
41. Tobin DM, Vary JC, Jr, Ray JP, Walsh GS, Dunstan SJ, Bang ND, Hagge DA, Khadge S, King MC, Hawn TR, Moens CB, Ramakrishnan L. 2010. The lta4h locus modulates susceptibility to mycobacterial infection in zebrafish and humans. Cell 140:717–730. https://doi.org/10.1016/j.cell.2010.02.013.
42. Rajan V, Dellaire G, Berman JN. 2016. Modeling leukemogenesis in the zebrafish using genetic and xenograft models. Methods Mol Biol 1451:171–189. https://doi.org/10.1007/978-1-4939-3771-4_12.
43. Wertman J, Veinotte CJ, Dellaire G, Berman JN. 2016. The zebrafish xenograft platform: evolution of a novel cancer model and preclinical

screening tool. Adv Exp Med Biol 916:289–314. https://doi.org/10.1007/978-3-319-30654-4_13.
44. Peters BM, Palmer GE, Nash AK, Lilly EA, Fidel PL, Jr, Noverr MC. 2014. Fungal morphogenetic pathways are required for the hallmark inflammatory response during Candida albicans vaginitis. Infect Immun 82:532–543. https://doi.org/10.1128/IAI.01417-13.
45. Urban CF, Reichard U, Brinkmann V, Zychlinsky A. 2006. Neutrophil extracellular traps capture and kill Candida albicans yeast and hyphal forms. Cell Microbiol 8:668–676. https://doi.org/10.1111/j.1462-5822.2005.00659.x.
46. Liu P, Wu X, Liao C, Liu X, Du J, Shi H, Wang X, Bai X, Peng P, Yu L, Wang F, Zhao Y, Liu M. 2014. Escherichia coli and Candida albicans induced macrophage extracellular trap-like structures with limited microbicidal activity. PLoS One 9:e90042. https://doi.org/10.1371/journal.pone.0090042.
47. Balish E, Wagner RD, Vazquez-Torres A, Jones-Carson J, Pierson C, Warner T. 1999. Mucosal and systemic candidiasis in IL-8Rh$^{-/-}$ BALB/c mice. J Leukoc Biol 66:144–150.
48. Deng Q, Harvie EA, Huttenlocher A. 2012. Distinct signalling mechanisms mediate neutrophil attraction to bacterial infection and tissue injury. Cell Microbiol 14:517–528. https://doi.org/10.1111/j.1462-5822.2011.01738.x.
49. Lee SK, Kim SD, Kook M, Lee HY, Ghim J, Choi Y, Zabel BA, Ryu SH, Bae YS. 2015. Phospholipase D2 drives mortality in sepsis by inhibiting neutrophil extracellular trap formation and down-regulating CXCR2. J Exp Med 212:1381–1390. https://doi.org/10.1084/jem.20141813.
50. Sai J, Raman D, Liu Y, Wikswo J, Richmond A. 2008. Parallel phosphatidylinositol 3-kinase (PI3K)-dependent and Src-dependent pathways lead to CXCL8-mediated Rac2 activation and chemotaxis. J Biol Chem 283:26538–26547. https://doi.org/10.1074/jbc.M805611200.
51. Bonnett CR, Cornish EJ, Harmsen AG, Burritt JB. 2006. Early neutrophil recruitment and aggregation in the murine lung inhibit germination of Aspergillus fumigatus conidia. Infect Immun 74:6528–6539. https://doi.org/10.1128/IAI.00909-06.
52. Goncalves AS, Appelberg R. 2002. The involvement of the chemokine receptor CXCR2 in neutrophil recruitment in LPS-induced inflammation and in Mycobacterium avium infection. Scand J Immunol 55:585–591. https://doi.org/10.1046/j.1365-3083.2002.01097.x.
53. Swamydas M, Gao JL, Break TJ, Johnson MD, Jaeger M, Rodriguez CA, Lim JK, Green NM, Collar AL, Fischer BG, Lee CC, Perfect JR, Alexander BD, Kullberg BJ, Netea MG, Murphy PM, Lionakis MS. 2016. CXCR1-mediated neutrophil degranulation and fungal killing promote Candida clearance and host survival. Sci Transl Med 8:322ra10. https://doi.org/10.1126/scitranslmed.aac7718.
54. Koh AY, Kohler JR, Coggshall KT, Van Rooijen N, Pier GB. 2008. Mucosal damage and neutropenia are required for Candida albicans dissemination. PLoS Pathog 4:e35. https://doi.org/10.1371/journal.ppat.0040035.
55. Vazquez-Torres A, Balish E. 1997. Macrophages in resistance to candidiasis. Microbiol Mol Biol Rev 61:170–192.
56. Soares MP, Teixeira L, Moita LF. 2017. Disease tolerance and immunity in host protection against infection. Nat Rev Immunol 17:83–96. https://doi.org/10.1038/nri.2016.136.
57. Naglik JR, Moyes DL, Wachtler B, Hube B. 2011. Candida albicans interactions with epithelial cells and mucosal immunity. Microbes Infect 13:963–976. https://doi.org/10.1016/j.micinf.2011.06.009.
58. Hopke A, Nicke N, Hidu EE, Degani G, Popolo L, Wheeler RT. 2016. Neutrophil attack triggers extracellular trap-dependent Candida cell wall remodeling and altered immune recognition. PLoS Pathog 12:e1005644. https://doi.org/10.1371/journal.ppat.1005644.
59. Renshaw SA, Loynes CA, Trushell DM, Elworthy S, Ingham PW, Whyte MK. 2006. A transgenic zebrafish model of neutrophilic inflammation. Blood 108:3976–3978. https://doi.org/10.1182/blood-2006-05-024075.
60. Ellett F, Pase L, Hayman JW, Andrianopoulos A, Lieschke GJ. 2011. mpeg1 promoter transgenes direct macrophage-lineage expression in zebrafish. Blood 117:e49–e56. https://doi.org/10.1182/blood-2010-10-314120.
61. Westerfield M. 2000. The zebrafish book. A guide for the laboratory use of zebrafish (Danio rerio). University of Oregon Press, Eugene, OR.
62. National Research Council. 2011. Guide for the care and use of laboratory animals, 8th ed. National Academies Press, Washington, DC.
63. Singer JT, Phennicie RT, Sullivan MJ, Porter LA, Shaffer VJ, Kim CH. 2010. Broad-host-range plasmids for red fluorescent protein labeling of gram-negative bacteria for use in the zebrafish model system. Appl Environ Microbiol 76:3467–3474. https://doi.org/10.1128/AEM.01679-09.
64. Hopke A, Wheeler RT. 2017. In vitro detection of neutrophil traps and post-attack cell wall changes in Candida hyphae. Bio-protocols 7:e2213. https://doi.org/10.21769/BioProtoc.2213.
65. Schindelin J, Arganda-Carreras I, Frise E, Kaynig V, Longair M, Pietzsch T, Preibisch S, Rueden C, Saalfeld S, Schmid B, Tinevez JY, White DJ, Hartenstein V, Eliceiri K, Tomancak P, Cardona A. 2012. Fiji: an open-source platform for biological-image analysis. Nat Methods 9:676–682. https://doi.org/10.1038/nmeth.2019.